OPEN ACCESS Freely available online

PLOS ONE

Mathematical Model of Bursting in Dissociated Purkinje Neurons

Michael D. Forrest*

Department of Computer Science, University of Warwick, Coventry, West Midlands, United Kingdom

Abstract

In vitro, Purkinje cell behaviour is sometimes studied in a dissociated soma preparation in which the dendritic projection has been cleaved. A fraction of these dissociated somas spontaneously burst. The mechanism of this bursting is incompletely understood. We have constructed a biophysical Purkinje soma model, guided and constrained by experimental reports in the literature, that can replicate the somatically driven bursting pattern and which hypothesises Persistent Na^+ current (I_{NaP}) to be its burst initiator and SK K^+ current (I_{SK}) to be its burst terminator.

Citation: Forrest MD (2013) Mathematical Model of Bursting in Dissociated Purkinje Neurons. PLoS ONE 8(8): e68765. doi:10.1371/journal.pone.0068765

Editor: Gennady Cymbalyuk, Georgia State University, United States of America

Received January 31, 2013; **Accepted** May 31, 2013; **Published** August 13, 2013

Funding: The author conducted this work in 2007 and was funded at the time by the Medical Research Council (MRC) of the UK, http://www.mrc.ac.uk/index.htm. The funders had no role in study design, data collection and analysis, decision to publish, or preparation of the manuscript. This work was reviewed by the author, and written up for journal publication, in 2012 (with no funding appropriated for this task).

Competing Interests: The author has declared that no competing interests exist.

* E-mail: mikeforrest@hotmail.com

Introduction

In vitro, without any synaptic input, Purkinje neurons can spontaneously fire action potentials in a repeating trimodal pattern that consists of tonic spiking, bursting and quiescence [1–6]. So, Purkinje cells have been observed to burst, as a component of the trimodal firing pattern. This bursting has been shown to be dendritically driven, by dendritic Ca^{2+} spikes [3], and has been modeled [6]. Purkinje cells also burst in response to Climbing fiber (CF) input; a CF input produces a Ca^{2+} spike in the dendrites and this propagates to, and produces a burst event (''complex spike'') at, the soma [7–10].

In vitro, Purkinje cell behaviour is sometimes studied in a dissociated soma preparation in which the dendritic projection has been cleaved. A fraction of these dissociated somas are quiescent whilst others spontaneously fire simple spikes [11] or spontaneously burst [12]. Given that this preparation has no dendrites, the drive to its bursting must be of somatic origin. Hence, this bursting must be distinct from the bursting in the trimodal pattern of firing, which has been shown to be dendritically driven [3,6]. Furthermore, it must be distinct from burst events in response to CF input, which have been shown to be dendritically driven [7–10]. Indeed, the bursting waveform of isolated Purkinje somata is distinct from the *stereotypical* waveform of dendritically driven bursts.

Dendritically driven bursts have an ongoing increase in firing rate and termination by a more rapid increase in firing rate, with a decrease in spike height. The burst rides upon a slow wave of depolarisation and ends with a rapid depolarization. This depolarization is followed by a rapid hyperpolarization that persists through the interburst interval [3,6]. By contrast, somatically driven bursts are without any systematic change in firing rate or spike height upon burst progression [12]. The burst's final spike height is not dramatically smaller and the burst does not ride upon a wave of depolarisation. In addition, somatically driven bursts tend to be shorter (two to four spikes per burst) than dendritically driven bursts (which can have hundreds of spikes per burst, although most typically have under ten).

The mechanism of the isolated soma's spontaneous bursting is incompletely understood. Swensen and Bean [12] studied bursts in this experimental preparation; but they parsed the ionic basis to an imposed, elicited burst produced upon a depolarising current injection. Hence, they did not focus upon spontaneous bursting; so, to what extent are their findings applicable to spontaneous bursting? Here we have constructed a biophysical Purkinje soma model, guided and constrained by the experimental findings of Swensen and Bean [12], which can replicate the somatically driven spontaneous, bursting pattern. This model provides an ionic basis to spontaneous bursting, in a dissociated Purkinje soma. It hypothesises Persistent Na^+ current (I_{NaP}) to be the burst initiator and SK K^+ current (I_{SK}) to be the burst terminator. Swensen and Bean [12] implicate the importance of an inward TTX-sensitive (Na^+) current and we go further in resolving this as I_{NaP}. We find that Fast Na^+ (I_{NaF}) or Resurgent Na^+ (I_{NaR}) cannot generate bursts.

Why do some dissociated Purkinje somas spontaneously fire simple spikes [11] rather than spontaneously burst [12]? Our model provides an explanation; higher BK and/or SK activation (which can be driven by greater P-type Ca^{2+} current flow, and elevated $[Ca^{2+}]_i$) switches a dissociated Purkinje soma from bursting to tonic spiking. So, the bursting mode is ''gated'' by the BK and SK currents, which are in turn ''gated'' by the P-type Ca^{2+} current (I_{CaP}).

An isolated Purkinje cell soma is a severely reduced system. Is its bursting mode an artefact of the isolated soma system? Or can it occur in the full Purkinje cell morphology? If so, does it occur *in vivo* and does it have a physiological role? We do not address the latter issues here. But we do use the model to propose that the full Purkinje cell morphology *can* express the same bursting form as that observed in isolated Purkinje somas. *In vitro*, if the P-type voltage-gated Ca^{2+} current (I_{CaP}) is pharmacologically blocked in a full Purkinje cell morphology, its inherent tonic or trimodal firing

pattern can be replaced with a phase of bursting and then a depolarisation block [1,2]. The waveform of this bursting is without the stereotypical change in firing rate/spike height, upon burst progression, that characterises dendritically generated bursting [3]. In fact, it is reported as similar to that observed in mechanically dissociated somas [3]. So, we suggest that this bursting is somatically driven. Our soma model can replicate this transition upon a P-type Ca^{2+} channel block: tonic firing to bursting (somatically driven waveform) and finally to depolarisation block.

We propose that cerebellar Purkinje cells have two distinct bursting modes – dendritically driven and somatically driven. The somatically driven bursting mode is observed in dissociated Purkinje somas and we use our model to propose that it can also be observed in full Purkinje cell morphologies, all be it in an artificial system – in cerebellar slices with the perfusion of a drug. We propose the possibility that Purkinje cells express a somatically driven bursting form under physiological conditions and utilise it in information coding.

Materials and Methods

Numerical simulations were performed with the NEURON 5.6 simulator [13], using its backward Euler integration method and 25 μs time steps. The model soma is a single cylindrical compartment with a length and diameter of 22 μm; its specific membrane capacitance (C_m) is 0.8 μF/cm^2 [14]. The soma has highly TEA sensitive (I_{K_fast}), moderately TEA sensitive (I_{K_mid}) and TEA insensitive (I_{K_slow}) voltage-gated K^+ currents, a BK voltage-and-Ca^{2+}-gated K^+ current (I_{BK}), a P-type Ca^{2+} current (I_{CaP}), a hyperpolarization activated cation current (I_H), a leak current (I_L) and an intracellular Ca^{2+} dynamics abstraction - all sourced from Khaliq et al. [11]. In addition, it has a Resurgent Na^+ current (I_{NaR}) (description from [15]), a T-type Ca^{2+} current (I_{CaT}) and a Fast Na^+ current (I_{NaF}) (descriptions from [16]). The model currents have equations and kinetic parameters as described in their source literature, but with the modification of current density values to those shown in Table 1. This isolated somatic compartment spontaneously fires in a simple spiking form, as many isolated Purkinje somata do. It can be switched to bursting (4 spikes per burst) by adding a Persistent Na^+ current (I_{NaP}, density = 4 mS/cm^2; description from [17]) and a SK Ca^{2+}-gated K^+ current (I_{SK}, density = 4 mS/cm^2; description from [18]).

All model parameters were established by prior literature (as referenced) except the current densities, which are ill constrained by published experimental data. These variables were tuned manually [19] by iteratively running the model with different current density values and observing which combination of these gave the best fit between real and model Purkinje soma output. We tuned the model manually because, drawing from our experience, we reasoned that with the reasonable number of parameters, and with the significant complexity/timeframe of the model behaviours sought, parameter optimization algorithms would struggle to converge upon a good solution. Principally, we tuned the model to replicate the characteristics of bursting in an isolated Purkinje soma [12].

Model equations

C_m is the membrane capacitance, I is the current, V is the membrane potential in mV as a dimensionless quantity, t is time, E_K is the reversal potential for K^+ (−88 mV), E_{Na} is the reversal potential for Na^+ (+60 mV), E_L is the reversal potential for the Leak current (−60 mV), E_h is the reversal potential for the hyperpolarisation activated cation current (−30 mV), T is temperature ($36^{\circ}C$) and g_{max} is the maximal conductance ("current density").

Table 1. Maximal current conductances in the model soma.

Current	Density (mS/cm^2)
Resurgent Na^+	156
Fast Na^+	0.1
P-type Ca^{2+}	0.52
T-type Ca^{2+}	0.1
BK K^+	72.8
Highly TEA sensitive K^+	41.6
Moderately TEA sensitive K^+	20.8
TEA insensitive K^+	41.6
I_H	1.04
Leak	0.52
Persistent Na^+	4
SK K^+	4

Without the inclusion of the two currents highlighted in grey (Persistent Na^+ current and SK K^+ current), the model soma fires tonic spikes. With their inclusion, at the densities presented, the model soma bursts.
doi:10.1371/journal.pone.0068765.t001

g_{max} values, for the different currents, are shown in Table 1.

m, h and z are Hodgkin-Huxley "particles"/gates [**30**]; for example, for the m Hodgkin-Huxley gate:

$$\frac{dm}{dt} = \frac{m_\infty - m}{\tau_m} \tag{1}$$

The voltage (and/or intracellular calcium) dependence of a Hodgkin-Huxley (H-H) current [**30**] can be expressed by stating, for each H-H gate (e.g. for the m gate), either $[m_\infty, \tau_m]$ OR $[\alpha_m, \beta_m]$. These entities are voltage (and/or intracellular calcium) dependent. The latter set can give the former set through the relations:

$$m_\infty = \alpha_m/(\alpha_m + \beta_m) \tag{2}$$

$$\tau_m = 1/(\alpha_m + \beta_m) \tag{3}$$

Master equation.

$$C_m \cdot \frac{dV}{dt} = -\left(I_{K\_fast} + I_{K\_mid} + I_{K\_slow} + I_{BK} + I_{CaT} + I_{CaP} + I_H + I_L + I_{NaR} + I_{NaF} + I_{NaP} + I_{SK}\right) \tag{4}$$

If I_{NaP} and I_{SK} are removed, then the model is switched from bursting to tonic spiking.

Highly TEA sensitive K+ current [11].

$$I_{K\_fast} = g_{max} \cdot m^3 \cdot h \cdot (V - E_K) \tag{5}$$

$$m_\infty = \frac{1}{\exp\left(-\frac{V - -24}{15.4}\right)} \tag{6}$$

$$\tau_m = \begin{cases} 0.000103 + \\ 0.0149 * \exp(0.035 * V) \ldots\ldots\ldots\ldots\ldots\ldots [V < -35mV] \\ 0.000129 + \\ 1/[\exp(\frac{V+100.7}{12.9}) + \exp(\frac{V-56}{-23.1})] \ldots\ldots [V \geq -35mV] \end{cases} \quad (7)$$

$$h_\infty = 0.31 + \frac{1-0.31}{\exp\left(-\frac{V--5.8}{-11.2}\right)} \quad (8)$$

$$\tau_h = \begin{cases} 1.22 * 10^{-5} + \\ 0.012 * \exp[-(\frac{V+56.3}{49.6})^2] \ldots\ldots\ldots\ldots\ldots\ldots [V \leq 0mV] \\ 0.0012 + \\ 0.0023 * \exp(-0.141 * V) \ldots\ldots\ldots\ldots\ldots\ldots [V > 0mV] \end{cases} \quad (9)$$

$qt = 3^{\frac{T-22}{10}}$; T is temperature in degrees centigrade (36). The time constants $[\tau_m; \tau_h]$ are divided by qt, in a modification to the original description [**11**], to account for temperature.

Moderately TEA sensitive K+ current [11].

$$I_{K\_mid} = g_{\max} \cdot m^4 \cdot (V - E_K) \quad (10)$$

$$m_\infty = \frac{1}{\exp\left(-\frac{V--24}{20.4}\right)} \quad (11)$$

$$\tau_m = \begin{cases} 0.000688 + 1/[\exp(\frac{V+64.2}{6.5}) + \\ \exp(\frac{V-141.5}{-34.8})] \ldots\ldots\ldots\ldots [V < -20mV] \\ 0.00016 + 0.0008 * \\ \exp(-0.0267 * V) \ldots\ldots\ldots\ldots\ldots\ldots\ldots [V \geq -20mV] \end{cases} \quad (12)$$

$qt = 3^{\frac{T-22}{10}}$; T is temperature in degrees centigrade (36). The time constant $[\tau_m]$ is divided by qt, in a modification to the original description [**11**], to account for temperature.

TEA insensitive K+ current [11].

$$I_{K\_slow} = g_{\max} \cdot m^4 \cdot (V - E_K) \quad (13)$$

$$m_\infty = \frac{1}{\exp\left(-\frac{V--16.5}{18.4}\right)} \quad (14)$$

$$\tau_m = 0.000796 + 1/[\exp(\frac{V+73.2}{11.7}) + \exp(\frac{V-306.7}{-74.2})] \quad (15)$$

$qt = 3^{\frac{T-22}{10}}$; T is temperature in degrees centigrade (36). The time constant $[\tau_m]$ is divided by qt, in a modification to the original description [**11**], to account for temperature.

P-type Ca2+ current [11].

$$I_{CaP} = g_{\max} * m * ghk \quad (16)$$

Goldman-Hodgkin-Katz (ghk) equation:

$$ghk = (4 * P_{Ca^{2+}}) * \frac{V \cdot F^2}{R \cdot T} * \frac{[Ca^{2+}]_i - [Ca^{2+}]_o * \exp\left(\frac{-2 \cdot F \cdot V}{R \cdot T}\right)}{1 - \exp\left(\frac{-2 \cdot F \cdot V}{R \cdot T}\right)} \quad (17)$$

P_{Ca}^{2+} is $5*10^{-5}$ cm/sec, $[Ca^{2+}]_i = 100$ nM, $[Ca^{2+}]_o = 2$ mM, T = 295 K, F is the Faraday constant and R is the gas constant. $[Ca^{2+}]_i$ and $[Ca^{2+}]_o$ are fixed constants, as seen by this equation – it does *not* access the changing value of $[Ca^{2+}]_i$ as set by the intracellular Ca^{2+} equations (given later).

$$m_\infty \frac{1}{\exp\left(-\frac{V--19}{5.5}\right)} \quad (18)$$

$$\tau_m = \begin{cases} 0.000264 + \\ 0.128 * \exp(0.103 * V) \ldots\ldots\ldots\ldots\ldots\ldots [V \leq -50mV] \\ 0.000191 + \\ 0.00376 * \exp[-(\frac{V+11.9}{27.8})^2] \ldots\ldots\ldots [V > -50mV] \end{cases} \quad (19)$$

$qt = 3^{\frac{T-22}{10}}$; T is temperature in degrees centigrade (36). The time constant $[\tau_m]$ is divided by qt, in a modification to the original description [**11**], to account for temperature.

Hyperpolarisation activated cation current [11].

$$I_H = g_{\max} \cdot m \cdot (V - E_h) \quad (20)$$

$$m_\infty = \frac{1}{\exp\left(-\frac{V--90.1}{-9.9}\right)} \quad (21)$$

$$\tau_m = 0.19 + 0.72 * \exp[-(\frac{V+81.5}{11.9})^2] \quad (22)$$

$qt = 3^{\frac{T-22}{10}}$; T is temperature in degrees centigrade (36). The time constant $[\tau_m]$ is divided by qt, in a modification to the original description [**11**], to account for temperature.

BK type K+ current [11].

$$I_{BK} = g_{\max} \cdot m^3 \cdot z^2 \cdot h \cdot (V - E_K) \quad (23)$$

$$m_\infty = \frac{1}{\exp\left(-\frac{V--28.9}{6.2}\right)} \quad (24)$$

$$h_\infty = 0.085 + \frac{1-0.085}{\exp\left(-\frac{V--32}{-5.8}\right)} \quad (25)$$

$$\tau_m = 0.000505 + 1/[\exp(\frac{V+86.4}{10.1}) + \exp(\frac{V-33.3}{-10})] \quad (26)$$

$$\tau_h = 0.0019 + 1/[\exp(\frac{V+48.5}{5.2}) + \exp(\frac{V-54.2}{-12.9})] \quad (27)$$

$$z_\infty = \frac{1}{1+\frac{0.001}{[Ca^{2+}]}} \quad (28)$$

$$\tau_z = 1 \quad (29)$$

$qt = 3^{\frac{T-22}{10}}$; T is temperature in degrees centigrade (36). The time constants $[\tau_m; \tau_h; \tau_z]$ are divided by qt, in a modification to the original description [**11**], to account for temperature.

Leak current [11].

$$I_L = g_{\max} * (V - E_L) \quad (30)$$

Intracellular Ca2+ concentration [11]. $[Ca^{2+}]$ is calculated for the intracellular space within 100 nm of the membrane. $[Ca^{2+}]$ changes as $I_{Ca}{}^{2+}$ brings Ca^{2+} into this space and as Ca^{2+} leaves by diffusion to the bulk cytoplasm. The diffusion rate constant, β, is set to 1/msec.

$$\frac{d[Ca^{2+}]}{dt} = \beta * [Ca^{2+}] \quad (31)$$

$[Ca^{2+}]$ at time step, t:

$$[Ca^{2+}]_t = [Ca^{2+}]_{t-1} + \Delta t * \left(\frac{-100 * I_{Ca2+}}{(2\cdot F) * (depth \cdot Area)} - \beta * [Ca^{2+}]_{t-1}\right) \quad (32)$$

F is the Faraday constant, $depth = 0.1\ \mu m$ and membrane surface $Area = 1{,}521\ \mu m^2$. $[Ca^{2+}]$ was constrained to not fall below 100 nM by coding of the form:

$$if([Ca^{2+}] < 100)\{[Ca^{2+}] = 100\}$$

Resurgent Na+ current [15].

$$I_{NaR} = g_{\max} * O * (V - E_{Na}) \quad (33)$$

O is the occupancy of the Open state.

This current is described by a Markov scheme, shown in Figure 1. The rate constants, labelled in Figure 1, are (ms^{-1}):

$$\alpha = 150 * \exp\left(\frac{V}{20}\right) \quad (34)$$

$$\beta = 3 * \exp\left(\frac{2\cdot V}{20}\right) \quad (35)$$

$\gamma = 150$; $\delta = 40$; $Con = 0.005$; $Coff = 0.5$; $Oon = 0.75$; $Ooff = 0.005$

$$a = \left(\frac{Oon}{Con}\right)^{1/4} \quad (36)$$

$$b = \left(\frac{Ooff}{Coff}\right)^{1/4} \quad (37)$$

$$\varepsilon = 1.75 \quad (38)$$

$$\zeta = 0.03 * \exp\left(\frac{2\cdot V}{25}\right) \quad (39)$$

All rate constants are multiplied by $qt = 3^{\frac{T-22}{10}}$; where T is temperature in degrees centigrade (36).

T-type Ca2+ current [16].

$$I_{CaT} = g_{\max} \cdot m \cdot h \cdot (V - E_{Ca}) \quad (40)$$

E_{Ca} is +135 mV for this current.

$$\alpha_m = \frac{2.6}{1+\exp\left(\frac{V+21}{-8}\right)} \quad (41)$$

$$\beta_m = \frac{0.18}{1+\exp\left(\frac{V+40}{4}\right)} \quad (42)$$

$$\alpha_h = \frac{0.0025}{1+\exp\left(\frac{V+40}{8}\right)} \quad (43)$$

$$\beta_h = \frac{0.19}{1+\exp\left(\frac{V+50}{-10}\right)} \quad (44)$$

$mt = 3^{\frac{T-37}{10}}$; T is temperature in degrees centigrade (36).

$$\tau_m = \frac{1}{(\alpha_m + \beta_m)\cdot mt} \quad (45)$$

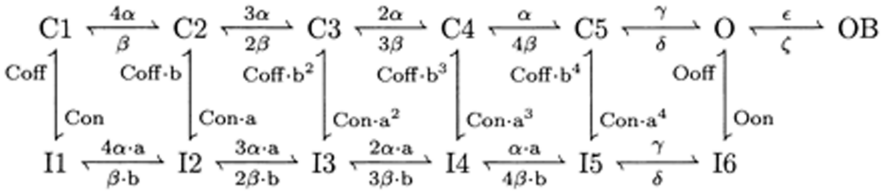

Figure 1. The Resurgent Na^+ current is described by a Markov scheme [11]. [C1 to C5] denote sequential Closed states; O denotes the Open state. [I1 to I6] denote Inactivated states. OB denotes the state entered by a second mechanism of inactivation, which is hypothesized to be equivalent to Open Channel Block. The rate constants between states are given in Eq. [34], Eq. [35], Eq. [36], Eq. [37], Eq. [38] and Eq. [39].
doi:10.1371/journal.pone.0068765.g001

$$\tau_h = \frac{1}{(\alpha_h + \beta_h)\cdot mt} \tag{46}$$

Fast Na+ current [16].

$$I_{NaF} = g_{\max}\cdot m^3\cdot h\cdot(V - E_{Na}) \tag{47}$$

E_{Na} is +45 mV for this current (as opposed to +60 mV).

$$\alpha_m = \frac{35}{0+\exp[\frac{V+5}{-10}]} \tag{48}$$

$$\beta_m = \frac{7}{0+\exp[\frac{V+65}{20}]} \tag{49}$$

$$\alpha_h = \frac{0.225}{1+\exp[\frac{V+80}{10}]} \tag{50}$$

$$\beta_h = \frac{7.5}{0+\exp[\frac{V+-3}{-18}]} \tag{51}$$

$mt = 3^{\frac{T-37}{10}}$; T is temperature in degrees centigrade (36).

$$\tau_m = \frac{1}{(\alpha_m + \beta_m)\cdot mt} \tag{52}$$

$$\tau_h = \frac{1}{(\alpha_h + \beta_h)\cdot mt} \tag{53}$$

Persistent Na+ current [17].

$$I_{NaP} = g_{\max}\cdot m\cdot(V - E_{Na}) \tag{54}$$

$$m_\infty = \frac{1}{1+\exp\left(\frac{-(V+42)}{5}\right)} \tag{55}$$

$$\alpha_m = \frac{0.091\cdot(V+42)}{1-\exp\left(\frac{-(V+42)}{5}\right)} \tag{56}$$

$$\beta_m = \frac{-0.062\cdot(V+42)}{1-\exp\left(\frac{-(V+42)}{5}\right)} \tag{57}$$

$ft = 3^{\frac{T-30}{10}}$; T is temperature in degrees centigrade (36).

$$\tau_m = \frac{5}{(\alpha_m + \beta_m)\cdot ft} \tag{58}$$

SK type K+ current [18].

$$I_{SK} = g_{\max}\cdot z^2\cdot(V - E_K) \tag{59}$$

$$z_\infty = \frac{48\cdot[Ca^{2+}]^2}{48\cdot[Ca^{2+}]^2 + 0.03} \tag{60}$$

$$\tau_z = \frac{1}{48\cdot[Ca^{2+}] + 0.03} \tag{61}$$

Results

The Purkinje soma model can replicate the somatically driven bursting pattern

Figure 2A shows a dendritically driven burst, of the trimodal firing pattern, from the full Purkinje cell model of Forrest et al. [6]. Figure 2B shows a somatically driven burst from our isolated soma model. Dendritically driven bursts have a very stereotypical waveform that contrasts with that of somatically driven bursts. They have an ongoing increase in firing rate and termination by a more rapid increase in firing rate, with a decrease in spike height. The burst rides upon a slow wave of depolarisation and ends with a rapid depolarization. This depolarization is followed by a rapid hyperpolarization that persists through the interburst interval [3,6]. By contrast, somatically driven bursts are without any systematic change in firing rate or spike height upon burst progression [12]. The burst's final spike height is not dramatically smaller and the burst does not ride upon a wave of depolarisation.

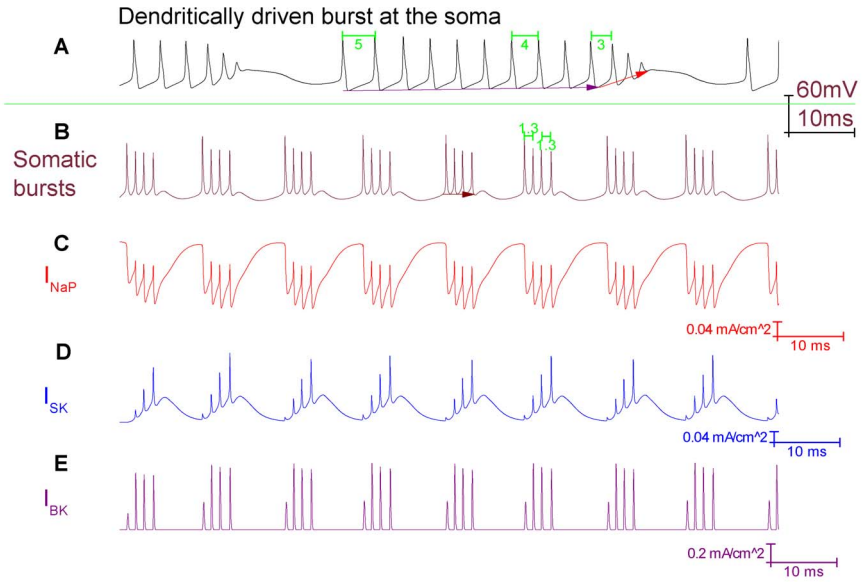

Figure 2. The isolated Purkinje soma model bursts if the I_{NaP} and I_{SK} conductances are both set to 4 mS/cm^2. These somatically driven bursts have a different waveform than dendritically driven bursts. *A*, Dendritically driven bursts in a full Purkinje cell model (described in [6]) have a very stereotypical waveform with an ongoing increase in firing rate and termination by a more rapid increase in firing rate, with a decrease in spike height. The former is highlighted by the labelled interspike intervals, which shorten upon burst progression. Each burst rides upon a slow wave of depolarisation (highlighted by the gradient of the blue arrow) and ends with a quick depolarization (highlighted by the gradient of the red arrow). It is followed by a rapid hyperpolarization that persists through the interburst interval. *B*, Somatically driven bursts in our isolated Purkinje soma model are, by contrast, without any systematic change in firing rate (refer to the labelled interspike intervals) or spike height upon burst progression and do not ride upon a wave of depolarisation (refer to the flat slope of the brown arrow). In addition, somatically driven bursts tend to be shorter (two to four spikes per burst) than dendritically driven bursts (which can have hundreds of spikes per burst, although more typically have under ten). *C*, I_{NaP} initiates and maintains the bursts in the Purkinje soma model. The Na^+ current conducted by the somatic I_{NaP} channel (following convention I_{NaP}, as an inward current, is represented as negative) is persistent and does not return to baseline after each spike in the burst. This persistence produces the sustained depolarization that initiates and maintains each somatic burst. *D*, I_{SK} is responsible for burst termination in the Purkinje soma model. During a burst, I_{SK} builds in magnitude until it ultimately attains enough strength to terminate it. I_{SK} then resets during the inter-burst interval. *E*, In contrast to I_{SK}, I_{BK} (except for an increase at the second spike) declines in magnitude with burst progression and is not responsible for burst termination. *Panel A and B scaling is encoded in the first scale bar (60 mV, 10 ms). Panel C scaling is encoded in the second scale bar (0.04 mA/cm^2, 10 ms). Panel D scaling is encoded in the third scale bar (0.04 mA/cm^2, 10 ms). Panel E scaling is encoded in the fourth scale bar (0.2 mA/cm^2, 10 ms).*
doi:10.1371/journal.pone.0068765.g002

In addition, somatically driven bursts tend to be shorter (two to four spikes per burst) than dendritically driven bursts (which can have hundreds of spikes per burst, although most typically have under ten).

Bursting in the Purkinje soma model: Persistent sodium current is the burst initiator; SK potassium current is the burst terminator

The isolated Purkinje soma model can be switched from spontaneous tonic firing, to spontaneous bursting, by the introduction of the Persistent Na^+ current (I_{NaP}, density = 4 mS/cm^2) and the SK Ca^{2+}-gated K^+ current (I_{SK}, density = 4 mS/cm^2).

The depolarising Persistent Na^+ current (I_{NaP}) produces the sustained depolarization that initiates and maintains a somatic burst: I_{NaP} is the "burst initiator" (*Figure 2C*). The hyperpolarising Ca^{2+}-activated SK potassium current (I_{SK}) builds in magnitude with burst progression, until it attains enough strength to terminate the burst, and produce the period of hyperpolarization before the next burst: I_{SK} is the burst "terminator" (*Figure 2D*). So, this bursting can be described as having a [I_{NaP} vs. I_{SK}] basis.

The Purkinje soma model was built with guidance from experimental findings

Swensen and Bean studied bursts in isolated Purkinje cell somas; they parsed the ionic basis to an imposed, elicited burst produced upon a depolarising current injection [12]. Our Purkinje soma model can burst spontaneously, without current injection. We set SK as the model's *spontaneous* burst terminator because Swensen and Bean have shown (experimentally) its importance to *elicited* somatic bursting: "SK increases progressively during bursts and plays an important role in regulating burst duration" [12]; SK is likely the burst terminator, and not BK, because "BK current progressively decreases during the burst, whereas SK current progressively increases" [12]. Our model replicates this rising SK current, and falling BK current, during burst progression (*Figure 2, panels D & E*).

We set a Na^+ current, rather than a Ca^{2+} current, as the depolarising force that initiates and maintains a somatically driven, *spontaneous* Purkinje burst because Na^+ channel block, by cobalt or TTX, prevents *elicited* bursting [12]. By contrast, Ca^{2+} channel block actually promotes *elicited* burst firing - "Blocking voltage-dependent Ca^{2+} entry by cadmium or replacement of external Ca^{2+} by Mg^{2+} enhanced burst firing" [12]. This promotion is likely manifested by Ca^{2+} channel block decreasing the intracellular Ca^{2+} concentration, which then results in less activation of the hypothesised burst terminator, the Ca^{2+}-activated SK channel.

So, by analogy with the experimental findings upon *elicited* somatic bursting, we hypothesise that the depolarising current that initiates and maintains *spontaneous* bursting is likely a Na^+ current. Manual tuning of Persistent Na^+ (I_{NaP}), Fast Na^+ (I_{NaF}) and Resurgent Na^+ (I_{NaR}) current densities showed only I_{NaP} able to

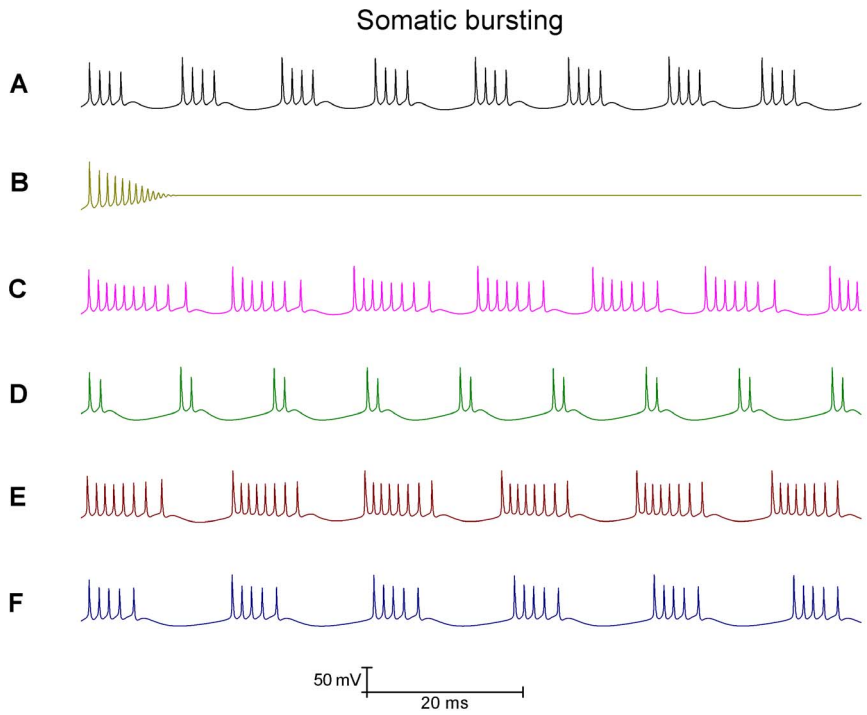

Figure 3. The bursting characteristics of the Purkinje soma model are dependent on a number of parameters. *A*, Bursts in the Purkinje soma model; I_{NaP} and I_{SK} have a current density of 4 mS/cm^2. *B*, I_{NaP} alone is not sufficient for bursting, I_{SK} is also required. With I_{NaP} present (the burst initiator) and I_{SK} absent (the burst terminator) a burst initiates but cannot terminate. So, the membrane potential becomes "stuck" mid-burst at a depolarised membrane potential. *C*, Increasing the I_{NaP} density (4 to 5 mS/cm^2) increases the number of spikes per burst (4 to 7). *D*, Increasing the I_{SK} density (4 to 8 mS/cm^2) decreases the number of spikes per burst (4 to 2). *E*, Increasing the I_{NaR} density (0.156 to 0.3 S/cm^2) increases the number of spikes per burst (4 to 7). *F*, Increasing the I_{CaT} density (0.1 to 1 mS/cm^2) increases the number of spikes per burst (4 to 5).
doi:10.1371/journal.pone.0068765.g003

generate spontaneous bursts in the model. With this modelling result, we hypothesise that I_{NaP} is the spontaneous burst initiator in real, dissociated Purkinje somas. I_{NaP} has been shown to be present in cerebellar Purkinje cells [20–22].

The hyperpolarisation activated cation current (I_H) contributes to bursting in a number of neuron types [23,24]. However, Swensen and Bean do not find it involved in *elicited* bursting, in isolated Purkinje somas [12]. Our modelling corresponds with this as I_H block (setting the I_H current density to 0) has no consequence upon *spontaneous* model bursting (data not shown).

Characteristics of bursting in the Purkinje soma model

1) I_{NaP} alone is not sufficient for bursting, I_{SK} is also required. If I_{NaP} (4 mS/cm^2) is introduced, without I_{SK}, then the model soma does not burst – it is depolarisation blocked. This is because the introduced I_{NaP} initiates a burst, but there is no I_{SK} to terminate it. So, the soma gets "stuck" mid-burst at a depolarised membrane potential (*Figure 3B*).
2) Increasing the density of the burst initiator, I_{NaP} (from 4 mS/cm^2 to 5 mS/cm^2), increases the number of spikes per burst (from 4 to 7) (*Figure 3C*).
3) Increasing the density of the burst terminator, I_{SK} (from 4 mS/cm^2 to 8 mS/cm^2), decreases the number of spikes per burst (from 4 to 2) (*Figure 3D*).
4) Increasing the density of Resurgent Na^+ current (I_{NaR}) (from 0.156 S/cm^2 to 0.3 S/cm^2) increases the number of spikes per burst (from 4 to 7). I_{NaR} is not the burst initiator and cannot generate bursting *de novo*. However, it can promote I_{NaP} established bursting (*Figure 3E*).
5) Increasing the density of the T-type Ca^{2+} current (I_{CaT}) (from 0.1 mS/cm^2 to 1 mS/cm^2) increases the number of spikes per burst (from 4 to 5). I_{CaT} is not the burst initiator and cannot generate bursting *de novo*. However, it can promote I_{NaP} established bursting (*Figure 3F*).

I_{BK} and/or I_{SK} activity can set whether the Purkinje soma model fires tonic spikes or bursts

1) Increasing the density of I_{SK} sufficiently (from 4 mS/cm^2 to 20 mS/cm^2) can switch the model out of bursting and into simple spiking (*Figure 4A*).
2) Increasing the density of I_{BK} sufficiently (from 0.0728 S/cm^2 to 10 S/cm^2) can switch the model out of bursting and into simple spiking (*Figure 4B*).
3) Increasing the density of both I_{SK} and I_{BK} (to 20 mS/cm^2 and 10 S/cm^2 respectively) can switch the model out of bursting and into simple spiking (*Figure 4C*). In this condition bursting is prevented by both I_{BK} and I_{SK} in a redundancy. Removing I_{BK} does not permit bursting because the I_{SK} block to bursting is still present (*Figure 4D*). Removing I_{SK} does not permit bursting because the I_{BK} block to bursting is still present (*Figure 4E*).

Bursting occurs when the depolarisation capacity exceeds the repolarisation capacity, and so the potential cannot be repolarised to the resting potential before the onset of the next spike. Raising I_{BK} and/or I_{SK} density, both repolarising entities, can correct this imbalance in the model and set a simple spiking pattern. Conceivably the raising of any repolarising current can act

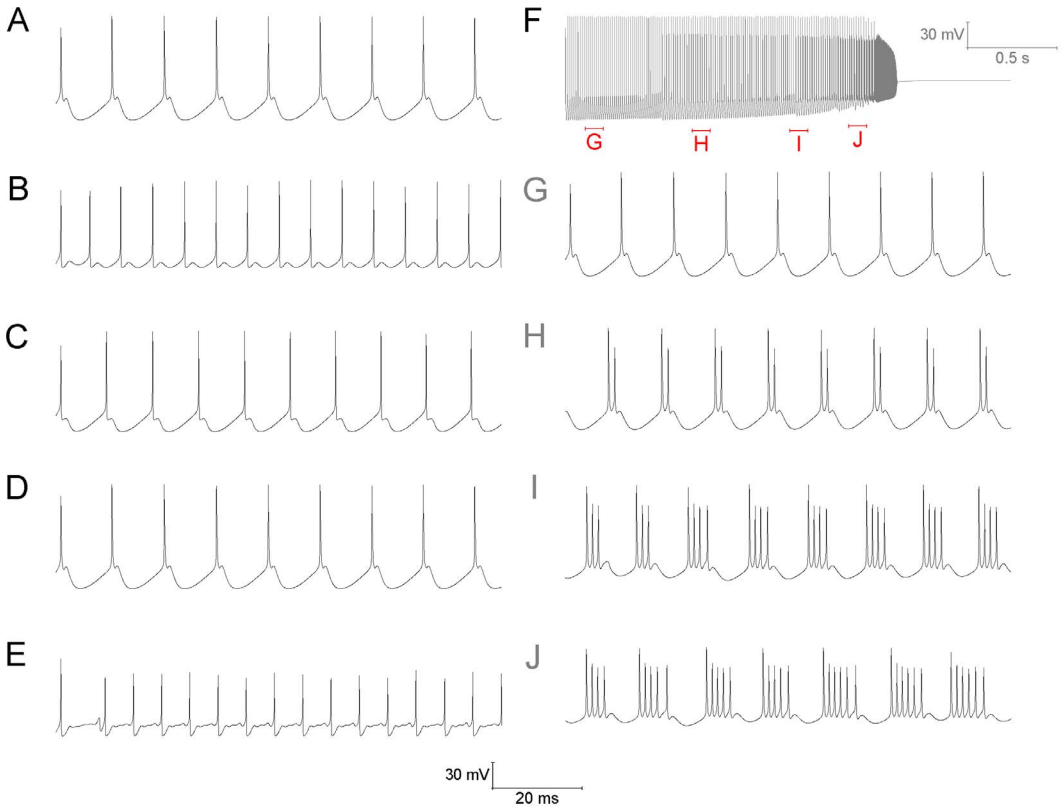

Figure 4. The bursting of the Purkinje soma model is gated by the BK and SK conductances. *A*, Increasing the I_{SK} density (4 to 20 mS/cm^2) switches the model from bursting to simple spiking. *B*, Increasing the I_{BK} density (0.0728 to 10 S/cm^2) switches the model from bursting to simple spiking. *C*, Increasing both the SK and BK densities (I_{SK} from 4 to 20 mS/cm^2. I_{BK} from 0.0728 to 10 S/cm^2) switches the model from bursting to simple spiking. In this condition bursting is prevented by both I_{BK} and I_{SK} in a redundancy. *D*, Removing I_{BK} does not permit bursting because the I_{SK} block to bursting is still present. *E*, Removing I_{SK} does not permit bursting because the I_{BK} block to bursting is still present. *F*, However, concurrent I_{BK} and I_{SK} removal does permit bursting. For example, decreasing the I_{BK} and I_{SK} densities to zero by an arbitrary function of time (t) [density(t) = density(0)-0.00001*t] shifts the somatic activity from simple spiking, into bursting and then depolarisation block silence. So, in this panel one can observe the transition from tonic spiking to bursting. *Panels G, H, I and J* correspond to the labelled parts of *Panel F* and highlight the transition from simple spiking to bursting. *Panel F scaling is encoded in its own scale bar (30 mV, 0.5 s); the scaling of all other panels is encoded in the scale at the bottom of the figure (30 mV, 20 ms).*
doi:10.1371/journal.pone.0068765.g004

similarly to switch bursting to simple spiking – to gate the bursting/simple spiking duality. However, we specifically hypothesise that real Purkinje somata have gating by both I_{BK} and I_{SK}. Hence for bursting to be "unlocked", both I_{BK} and I_{SK} activation must be reduced. We arrive at this hypothesis from an interpretation of experimental data in the literature.

If the P-type voltage-gated Ca^{2+} current (I_{CaP}) is pharmacologically blocked in a full Purkinje cell morphology, its inherent trimodal (or tonic) firing pattern can be eventually replaced with a phase of bursting and then a depolarisation block [1,2]. The waveform of this bursting is without the stereotypical change in firing rate/spike height, upon burst progression, that characterises dendritically generated bursting [3]. It is reported as similar to that observed in mechanically dissociated somas [3]. So, we hypothesise that this bursting is somatically driven and corresponds to the bursting observed in some isolated Purkinje somata [12]. Thus, we believe its study can be used to derive insight into the bursting of isolated somata bursting, and vice-versa.

We hypothesise that I_{CaP} block causes this outcome (bursting and then depolarisation block) because it equates to a combined I_{BK} and I_{SK} block. BK and SK channel activation is selectively coupled to I_{CaP} activation - experiments have shown that Ca^{2+} for activating BK and SK channels is provided *solely* by I_{CaP} flow in the Purkinje cell [2] i.e. BK and SK channels do not "read" the global intracellular Ca^{2+} concentration but singly the Ca^{2+} flux through I_{CaP}. The concurrent reduction in BK and SK activity unlocks the somatic bursting state. Then, during this bursting mode, as the proportion of I_{CaP} molecules that are blocked increases over time, the BK and SK activity level falls further still. As SK activity falls, eventually SK cannot fulfill its role as the "burst terminator" and a burst cannot be terminated and a depolarisation block silence ensues. I_{CaP} block ensures a concurrent reduction in BK and SK activity: the individual block of BK or SK cannot switch a Purkinje cell out of the trimodal (or tonic) firing pattern [2,4].

Figure 4F shows the effect of decreasing the I_{BK} and I_{SK} densities to zero, with an arbitrary function of time (t) [density(t) = density(0) - $(1*10^{-5})$*t] that abstracts a progressing pharmacological block of BK and SK. It shifts the somatic model activity from simple spiking, into bursting and then depolarisation block silence. Figure 5 shows the effect of decreasing the I_{CaP} density to zero, with an arbitrary function of time (t) [density(t) = density(0) - $(1*10^{-7})$*t] that abstracts a progressing pharmacological block of I_{CaP}. It shifts the somatic model activity from simple spiking, into bursting and then depolarisation block silence. The reduction in

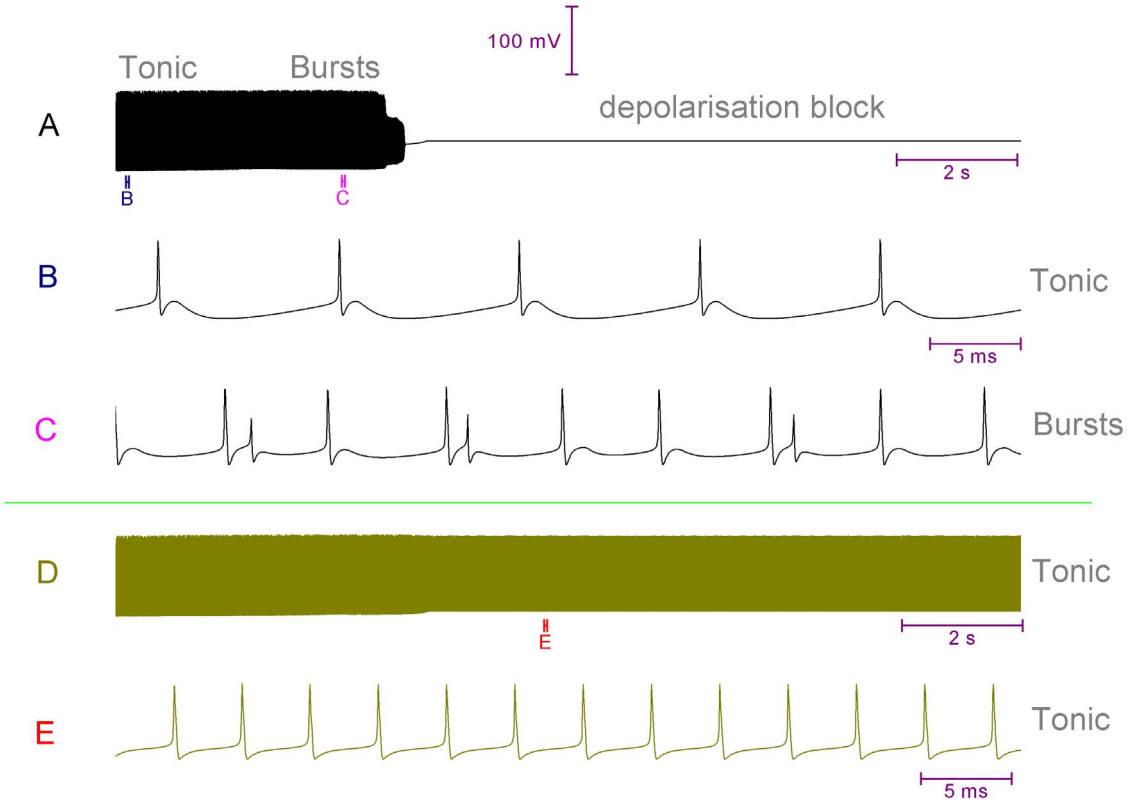

Figure 5. The bursting of the Purkinje soma model is gated by I_{CaP}. *A*, Decreasing the I_{CaP} density to zero, with an arbitrary function of time (t) [density(t) = density(0) - $(1*10^{-7})$*t], shifts the somatic model activity from simple spiking, into bursting and then depolarisation block silence. *Panels B and C* correspond to the labelled parts of *Panel A* and highlight the transition from simple spiking to bursting. The bursting is irregular, with doublets interspersed with single spikes, as has been observed in some experimental recordings of somatic bursting [**12**]. *D*, I_{CaP} reduction can only unmask somatic bursting if the foundations for it are existent i.e. I_{NaP} and I_{SK} are both present at sufficient densities. If not, for example if the I_{NaP}, density = 0 mS/cm^2, then I_{CaP} reduction does not switch the somatic model out of tonic firing and the tonic firing state persists indefinitely. *Panel E* corresponds to the labelled part of *Panel D. All panels are scaled in the y axis (membrane potential) by the same scale bar, at the top of the figure (100 mV). Each panel has its own scale bar for the x axis (time).*
doi:10.1371/journal.pone.0068765.g005

the I_{CaP} density causes this same switch in behaviour because it causes a concurrent decrease in I_{BK} and I_{SK} activity.

Note that I_{CaP} block (or I_{BK} and I_{SK} block) can only unmask somatic bursting if the foundations for it are existent: if I_{NaP} and I_{SK} (the burst initiator and terminator) are both present at sufficient densities. If not then I_{CaP} block (or I_{BK} and I_{SK} block) does not switch the soma model out of tonic firing and the tonic firing state persists indefinitely (Figure 5D & 5E).

The Purkinje soma model can replicate Swensen and Bean's [12] elicited burst protocol

For most of their study, Swensen and Bean [12] perform experiments upon an artificial form of somatic bursting. They take an isolated soma that spontaneously fires simple spikes and hold it at a hyperpolarised silence (−90 mV) with an enduring, hyperpolarising current injection. This "held" cell is then driven to fire a single burst by a very short (1 ms) depolarising current injection. Although the cell intrinsically generates simple spikes it fires a burst in this protocol. Hence the studied burst is elicited rather than spontaneous. This raises the concern that the mechanisms elucidated for the generation of such an elicited burst are not relevant for spontaneous bursts. Modelling can help address this issue. Our model's spontaneous bursting mechanism (I_{NaP} vs. I_{SK}) primarily comes from an analysis of observations that Swensen and Bean [12] made for elicited bursts. Indeed, this mechanism allows the model to replicate their elicited burst results (*Figure 6*). But importantly, it also allows the model to fire bursts spontaneously. This demonstrates that elicited and spontaneous bursts are likely to have an equivalent basis, which vindicates the value of experiments that employ the elicited burst protocol.

Discussion

An isolated Purkinje cell soma is a severely reduced system, but it is used in experimental research [11,12]. In this paper we propose a biophysical basis to its bursting mode; Persistent Na^+ current (I_{NaP}) is the burst initiator and SK K^+ current (I_{SK}) is the burst terminator. This bursting mode is "gated" by the BK and SK currents (in a redundancy), which are in turn "gated" by the P-type Ca^{2+} current.

Is this bursting mode an artefact of the isolated soma system, or does it relate to physiological processes? Well, this bursting does not correspond to the bursting observed in the trimodal pattern of activity, in the full Purkinje cell morphology, because this bursting is dependent on the dendrites [3]. However, we suggest that the full Purkinje cell morphology can express the same bursting form as that observed in isolated Purkinje somata. This is, *in vitro*, upon the condition of P-type Ca^{2+} channels being pharmacologically blocked [1,3]. So, this expression is itself in a severely artificial

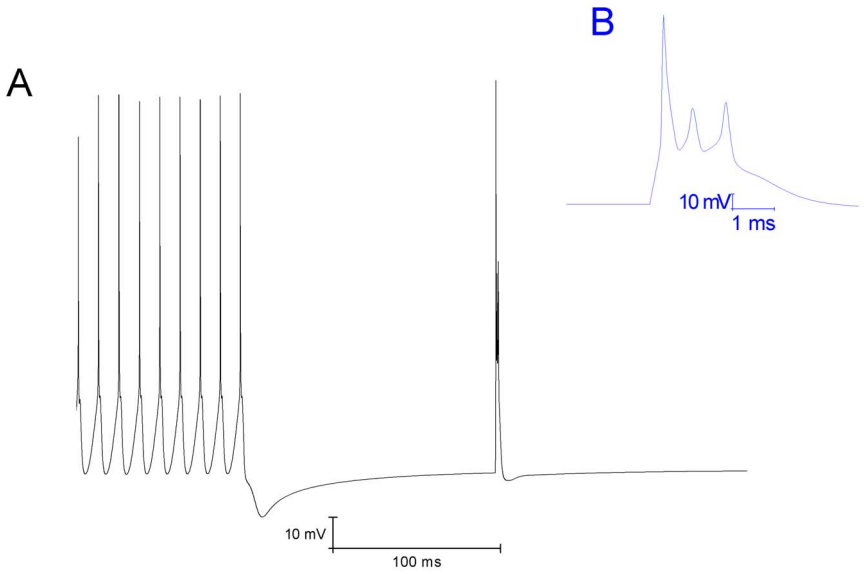

Figure 6. The Purkinje soma model can replicate Swensen and Bean's [12] elicited burst protocol. *A*, The model soma spontaneously fires simple spikes because it has an elevated I_{BK} and I_{SK} density that blocks bursting. At 100 ms it is driven to a hyperpolarised silence, and held there, by a maintained hyperpolarising current injection (−0.5 nA). This "held" cell is then driven to fire a single burst by a very short (1 ms) depolarising current injection (2 nA). Although the cell intrinsically fires simple spikes, it fires a burst in this protocol. So, the studied burst is elicited rather than spontaneous. *B*, The elicited burst at higher resolution.
doi:10.1371/journal.pone.0068765.g006

system: in cerebellar slices with the perfusion of a drug. There is presently no work that we know of that investigates or supports the hypothesis that, physiologically, Purkinje cells express a somatically driven bursting form and utilise it in information coding strategies. However, if they do employ this firing form, we can speculate that its bursting parameters might be under transmitter control as a computational feature. Transmitter control of I_{SK} has been described in many types of neurons [25], I_{NaR} may be regulated by phosphorylation [26] and I_{NaP} can be regulated by Nitric Oxide [27], Protein Kinase C [28] and external Ca^{2+} concentration [29].

In this paper, we have proposed the electrophysiological basis to bursting in an isolated Purkinje soma. We have shown how it could relate to different activity patterns that have been reported in full Purkinje cell morphologies [1,3], and in isolated Purkinje somas [11], by other scientists in other experiments. This is the value of modelling – it can reconcile why different behaviour is observed in different experimental preparations and unify disparate behaviour into a single, cohesive framework.

In conclusion, we propose that the Purkinje cell has two separate and distinct modes of bursting: somatically generated and dendritically generated, which have dramatically different waveforms. We venture that the Purkinje cell may leverage this in its information coding strategies.

Author Contributions

Conceived and designed the experiments: MDF. Performed the experiments: MDF. Analyzed the data: MDF. Contributed reagents/materials/analysis tools: MDF. Wrote the paper: MDF.

References

1. Womack M, Khodakhah K (2002) Active contribution of dendrites to the tonic and trimodal patterns of activity in cerebellar Purkinje neurons. J Neurosci 22:10603–10612.
2. Womack MD, Chevez C, Khodakhah K (2004) Calcium-activated potassium channels are selectively coupled to P/Q-type calcium channels in cerebellar Purkinje neurons. J Neurosci 24(40):8818–22.
3. Womack MD, Khodakhah K (2004) Dendritic control of spontaneous bursting in cerebellar Purkinje cells. J Neurosci 24:3511–3521.
4. Womack MD, Khodakhah K (2003) Somatic and dendritic small conductance calcium-activated potassium channels regulate the output of cerebellar Purkinje neurons. J Neurosci 23:2600–2607.
5. McKay BE, Turner RW (2005) Physiological and morphological development of the rat cerebellar Purkinje cell. J Physiol 567: 829–850.
6. Forrest MD, Wall MJ, Press DA, Feng J (2012) The Sodium-Potassium Pump Controls the Intrinsic Firing of the Cerebellar Purkinje Neuron. PLoS ONE 7(12): e51169. doi:10.1371/journal.pone.0051169.
7. Knöpfel T, Vranesic I, Staub C, Gähwiler BH (1991) Climbing Fibre Responses in Olivo-cerebellar Slice Cultures. II. Dynamics of Cytosolic Calcium in Purkinje Cells. Eur J Neurosci 3(4):343–348.
8. Llinás R, Sugimori M (1980b) Electrophysiological properties of in vitro Purkinje cell dendrites in mammalian cerebellar slices. J Physiol 305:197–213.
9. Miyakawa H, Lev-Ram V, Lasser-Ross N, Ross WN (1992) Calcium transients evoked by climbing fiber and parallel fiber synaptic inputs in guinea pig cerebellar Purkinje neurons. J Neurophysiol 68(4):1178–89.
10. De Schutter E, Bower JM (1994) An active membrane model of the cerebellar Purkinje cell II. Simulation of synaptic responses. J Neurophysiol 71:401–19.
11. Khaliq ZM, Gouwens NW, Raman IM (2003) The contribution of resurgent sodium current to high-frequency firing in Purkinje neurons: an experimental and modeling study. J Neurosci 23:4899–4912.
12. Swensen AM, Bean BP (2003) Ionic mechanisms of burst firing in dissociated Purkinje neurons. J Neurosci 23:9650–9663.
13. Hines ML, Carnevale NT (1997) The NEURON simulation environment. Neural Comput 9:1179–1209.
14. Miyasho T, Takagi H, Suzuki H, Watanabe S, Inoue M, et al. (2001) Low-threshold potassium channels and a low-threshold calcium channel regulate Ca^{2+} spike firing in the dendrites of cerebellar Purkinje neurons: a modeling study. Brain Res 891:106–15.
15. Akemann W, Knopfel T (2006) Interaction of Kv3 potassium channels and resurgent sodium current influences the rate of spontaneous firing of Purkinje neurons. J Neurosci 26:4602–4612.
16. De Schutter E, Bower JM (1994a) An active membrane model of the cerebellar Purkinje cell. I. Simulation of current clamps in slice. J Neurophysiol 71:375–400.
17. D'Angelo E, Nieus T, Maffei A, Armano S, Rossi P, et al. (2001) Theta-frequency bursting and resonance in cerebellar granule cells: experimental evidence and modeling of a slow k+-dependent mechanism. J Neurosci 21:759–70.
18. Destexhe A, Contreras D, Sejnowski TJ, Steriade M (1994) A model of spindle rhythmicity in the isolated thalamic reticular nucleus. J Neurophysiol 72:803–18.

19. Prinz A (2006) Neuronal parameter optimization. Scholarpedia, 2(1):1903.
20. Llinas R, Sugimori M (1980a) Electrophysiological properties of in vitro Purkinje cell somata in mammalian cerebellar slices. J Physiol (Lond) 305:171–195.
21. Vega-Saenz de Miera EC, Rudy B, Sugimori M, Llinas R (1997) Molecular characterization of the sodium channel subunits expressed in mammalian cerebellar Purkinje cells. Proc Natl Acad Sci USA 94:7059–7064.
22. Kay AR, Sugimori M, Llinas R (1998) Kinetic and stochastic properties of a persistent sodium current in mature guinea pig cerebellar Purkinje cells. J Neurophysiol 80:1167–1179.
23. Pape HC (1996) Queer current and pacemaker: the hyperpolarization activated cation current in neurons. Annu Rev Physiol 58:299–327.
24. Luthi A, Bal T, McCormickDA (1998) Periodicity of thalamic spindle waves is abolished by ZD7288, a blocker of *I*h. J Neurophysiol 79:3284–3289.
25. Nicoll RA (1988) The coupling of neurotransmitter receptors to ion channels in the brain. Science 241:545–551.
26. Grieco TM, Afshari FS, Raman IM (2002) A role for phosphorylation in the maintenance of resurgent sodium current in cerebellar Purkinje neurons. J Neurosci 22:3100–3107.
27. Hammarstrom AK, Gage PW (1999) Nitric oxide increases persistent sodium current in rat hippocampal neurons. J Physiol (Lond) 520:451–461.
28. Alroy G, Su H, Yaari Y (1999) Protein kinase C mediates muscarinic block of intrinsic bursting in rat hippocampal neurons. J Physiol (Lond) 517:71–79.
29. Su H, Alroy G, Kirson ED, Yaari Y (2001) Extracellular calcium modulates persistent sodium current-dependent burst-firing in hippocampal pyramidal neurons. J Neurosci 21:4173–4182.
30. Hille B (2001) Ion channels of excitable membranes. Sunderland, MA: Sinauer.